HHS Public Access

Author manuscript

Bone. Author manuscript; available in PMC 2021 February 01.

Published in final edited form as:

Bone. 2020 February ; 131: 115151. doi:10.1016/j.bone.2019.115151.

Hypophosphatemic Rickets Accelerate Chondrogenesis and Cell Trans-differentiation from TMJ Chondrocytes into Bone Cells via a Sharp Increase in β-Catenin

Hui Li[1,2], **Yan Jing**[3], **Rong Zhang**[1], **Qi Zhang**[1,4], **Jun Wang**[1,2], **Aline Martin**[5], **Jian Q. Feng**[1]

[1]Department of Biomedical Sciences, Texas A&M University College of Dentistry, Dallas, Texas 75246, U.S.A.

[2]State Key Laboratory of Oral Diseases, Department of Traumatic and Plastic Surgery, West China Hospital of Stomatology, Sichuan University, Chengdu 610041, China.

[3]Department of Orthodontics, Texas A&M University College of Dentistry, Dallas, TX, 75246, USA.

[4]Laboratory of Oral Biomedical Science and Translational Medicine, Department of Endodontics, School of Stomatology, Tongji University, Shanghai, China

[5]Center for Translational Metabolism and Health, Division of Nephrology/Hypertension, Feinberg School of Medicine, Northwestern University, Chicago, IL, 60611, USA.

Abstract

Dentin matrix protein 1 (DMP1) is primarily expressed in osteocytes, although a low level of DMP1 is also detected in chondrocytes. Removing *Dmp1* in mice or a mutation in humans leads to hypophosphatemic rickets (identical to X-linked hypophosphatemia). The deformed skeletons were currently thought to be a consequence of an inhibition of chondrogenesis (leading to an accumulation of hypertrophic chondrocytes and a failure in the replacement of cartilage by bone). To precisely study the mechanisms by which DMP1 and phosphorus control temporomandibular condyle formation, we first showed severe malformed condylar phenotypes in Dmp1-null mice (great expansions of deformed cartilage layers and subchondral bone), which worst as aging. Next, we excluded the direct role of DMP1 in condylar hypertrophic-chondrogenesis by conditionally deleting Dmp1 in hypertrophic chondrocytes using Col10a1-Cre and Dmp1 loxP mice (displaying no apparent phosphorous changes and condylar phenotype). To address the mechanism by which the onset of endochondral phenotypes takes place, we generated two sets of tracing lines in the

Corresponding authors: Jian Q. Feng, jfeng@tamu.edu;.

AUTHOR CONTRIBUTIONS

H. Li contributed to conception, design, data acquisition, analysis, and interpretation, drafted the manuscript; Y. Jing contributed to data interpretation, drafted and revised the manuscript; Rong Zhang contributed to data acquisition, analysis, and interpretation; Qi Zhang contributed to data acquisition, analysis, and interpretation; Jun Wang contributed to data interpretation, revised the manuscript; A. Martin contributed to data acquisition, analysis, and interpretation; J.Q.Feng, contributed to conception, design, and data interpretation, drafted and critically revised the manuscript. All authors gave final approval and agree to be accountable for all aspects of the work.

Dmp1 KO background: AggrecanCreERT2-ROSA-tdTomato and Col 10a1-Cre-ROSA-tdTomato, respectively. Both tracing lines displayed an acceleration of chondrogenesis and cell trans-differentiation from chondrocytes into bone cells in the Dmp1 KO. Next, we showed that administrations of neutralizing fibroblast growth factor 23 (FGF23) antibodies in *Dmp1*-null mice restored hypophosphatemic condylar cartilage phenotypes. In further addressing the rescue mechanism, we generated compound mice containing Col10a1-Cre with ROSA-tdTomato and *Dmp1* KO lines with and without a high Pi diet starting at day 10 for 39 days. We demonstrated that hypophosphatemia leads to an acceleration of chondrogenesis and trans-differentiation of chondrocytes to bone cells, which were largely restored under a high Pi diet. Finally, we identified the causative molecule (β-catenin). Together, this study demonstrates that the *Dmp1*-null caused hypophosphatemia, leading to acceleration (instead of inhibition) of chondrogenesis and bone trans-differentiation from chondrocytes but inhibition of bone cell maturation due to a sharp increase in β-catenin. These findings will aid in the future treatment of hypophosphatemic rickets with FGF23 neutralizing antibodies.

Keywords

DMP1; hypophosphatemic rickets; FGF 23; cell lineage tracing; mandibular condyle

1. INTRODUCTION

Dentin matrix protein 1 (DMP1) is non-collagenous phosphoprotein that belongs to the small integrin binding ligand, N-linked glycoproteins (SIBLING) family [1–3]. Although originally isolated from a rat incisor, DMP1 is highly expressed in osteocytes that account for more than 90% of bone cells [4–6]. The presence of DMP1 is critical for normal postnatal chondrogenesis and subsequent osteogenesis [7]. Mutations of *Dmp1* in humans [5, 7], and deletion of *Dmp1* in mice [8] or in rabbits [9] leads to abnormality in osteocyte maturation and an increase of fibroblast growth factor 23 (FGF23), a key factor for Autosomal Recessive Hypophosphatemic Rickets type I (ARHR1, OMIM 241520). It is known that FGF23, a phosphaturic hormone produced by osteocytes, inhibits renal phosphate reabsorption and 1, 25-dihydroxyvitamin D synthesis, resulting in hypophosphatemia manifested by rickets and osteomalacia [10–12]. The anti-FGF23 antibody has been successfully used in treatment of hypophosphatemic rickets patients [13, 14], and restored *Dmp1 KO* long bone phenotype in mice [15]. Now, anti-FGF23 antibody, Burosumab, is recently approved by the US FDA, and Health Canada as well as conditionally approved by the European Medicines Agency for treatment of adults and children with X-linked hypophosphatemia (XLH) [16].

For decades, hypertrophic chondrocytes have been widely thought to undergo apoptosis prior to the invasion of bone marrow-derived mesenchymal cells. However, recent evidences demonstrated that chondrocytes can directly transform into bone cells [17–19]. Furthermore, a new hypothesis was raised: chondrogenesis and osteogenesis are one continuous biological process instead of two separate processes during endochondral bone ossification [20].

The cartilage of the mandibular condyle, distinct from other cartilage of limb joints, is derived from cranial neural crest cells [21]. Importantly, the articular surface of the mandibular condyle is covered by fibrocartilage, in which there is a high level of collagen type VI [22]. Current studies have focused on the role of DMP1 and phosphorus in limb bone formation, with little attention to the function of DMP1 in condyle growth.

In this study, we intend to investigate the roles of DMP1 and phosphorus in condyle development. Using conventional and conditional *Dmp1* knockout (KO) models, and four compound mouse lines including *Dmp1* KO with Acan-Cre^{ERT2}; R26R^{Tomato} cell lineage, Col10a1-Cre; R26R^{Tomato} cell lineage, Col10a1-Cre; *Dmp1*-loxP mice, and Acan-Cre^{ERT2}; β-catenin flox$^{(Ex3)}$/flox$^{(Ex3)}$; R26R^{Tomato} mice. We demonstrated that the loss of DMP1 leads to a severe defect of condyle development and remodeling. We also showed a lack of the direct role of DMP1 in condyle hypertrophic-chondrogenesis but a great impact of phosphorus on the KO condyle. Critically, we demonstrated a sharp increase in acceleration of chondrogenesis (instead of the inhibition of chondrogenesis as commonly believed) and a cell trans-differentiation from chondrocytes to bone cells, a great reduction of extracellular matrix secretion due to an increase in β-catenin caused by a low phosphorus level. Finally, administrations of the anti-FGF23 neutralizing antibodies or a high Pi diet greatly improve the above phenotypes. Our new findings challenge the current view on the onset of hypophosphatemic rickets in the mandibular condyle.

2. Materials and methods

2.1. Breeding transgenic mice

Dmp1 KO mice with exon 6 deletion and conditional allele of *Dmp1* mice were generated as previously described [6, 23]. To generate triple mice to specifically trace the cell face of hypertrophic chondrocytes, *Dmp1* KO, and R26R^{Tomato} (B6;129S6-Gt(ROSA)26Sortm9(CAG-tdTomato)Hze/J, stock number: 007905 from the Jackson Laboratory) were internally crossed with Col10a1-Cre line [24]. Col10a1-Cre mice were crossed to *Dmp1*-loxP [25] for a specific deletion of *Dmp1* in hypertrophic chondrocytes. Similarly, *Dmp1* KO, R26R^{Tomato} and Acan-Cre^{ERT2} (one-time tamoxifen injection at day3, injection concentration;10mg/ml, 75 mg/kg body weight; 7.5μl /1gm of body weight) were generated to trace a chondrocyte cell fate. Tamoxifen (Sigma, T5648) was dissolved in 90% corn oil (Sigma, C8267) and 10% ethanol [26]. In order to constitutively active β-catenin in chondrocytes, β-catenin^{flox} [27], R26R^{Tomato} and Acan-Cre^{ERT2} (one time tamoxifen injection at day3 P3, 7.5μl /1gm of body weight) were internally crossed three times [26]. Age-matched wild type (WT) and heterozygous mice were used as controls because no obvious difference was found between them [5]. These mice were fed with autoclaved rodent chow (5010; Ralston Purina, St. Louis, MO, USA) containing 1% calcium, 0.67% phosphorus and 4.4 international units (IU) vitamin D/g (regular diet). To rescue the *Dmp1* KO mice, the animals were fed a rescue chow (Harlan Teklad, cat. TD.87133) containing 2% phosphorus, 1.1% calcium and 2.2 IU/g vitamin D from the age of 10-day to 7-week. Before pups were weaned, a high Pi diet was used to feed their mothers to keep a high Pi level. Right after weaned, all pups were fed with the same high-Pi diet. Administrations of the anti-FGF23 neutralizing antibodies were performed as previously described [15]. All

experimental procedures were performed in accordance with the Institutional Animal Care and Use Committee of Texas A&M University, College of Dentistry (Dallas, TX, USA).

2.2. Radiographs and micro-computed tomography (μCT) scanning

X-ray images of the mandibles at the same age were taken by a Faxitron model MX-20 Specimen Radiography System (Faxitron X-Ray Corp., Lincolnshire, IL, USA) [8].

The mandibular condyles from Control, KO, Control+High-Pi, and KO+High-Pi mice were scanned by Scanco μCT35 (Scanco Medical, Bassersdorf, Switzerland). For quantitative evaluation of the condylar bone, the area from the calcified cartilage to subchondral bone with a thickness of 1.5 mm (100 μCT slices) were selected and analyzed at a threshold of 220 mg/cm3. The following are the key parameters of the μCT scan: voxel size 6 μm, X-ray tube potential 55 kVp, X-ray intensity 145 μA, integration time 600 ms. Bone mineral density (BMD), Tb. N, and Tb. Sp were calculated and used for comparison between the samples.

2.3. Histological analysis and immunohistochemistry

For histological staining, mandibular condyles were fixed by freshly prepared 4% paraformaldehyde in PBS (pH 7.4) overnight, decalcified in 15% EDTA at 4°C, and embedded in paraffin as described previously [8, 28]. The samples were cut at 4.5 μm thickness and stained with Toluidine blue, Safranin-O fast green, Sirius Red and immunohistochemistry (IHC) staining as previously reported [15, 29]. Bioquant Osteo software was used for histological analysis (Bioquant Image Analysis Corporation, Nashville, TN, USA) in accordance with the American Society for Bone and Mineral Research [30]. Samples for cell lineage tracing, decalcified condyles were followed by CryoJane frozen sections as previously described [31].

The concentrations of primary antibodies for the immunohistochemistry are: rabbit anti-collagen X antibody (Abcam; 1:100), rabbit polyclonal anti-Sox9 (Santa Cruz Biotechnology; 1:100), rabbit polyclonal anti-Col 1 (Abcam; 1:100), rabbit anti-Runx2 antibody (Abcam; 1:50), goat polyclonal anti-sclerostin (SOST) (R&D ; 1:50), anti-β-catenin mouse monoclonal antibody (DSHB; PY489-B-catenin, specific to beta-catenin phosphorylated at Tyr 489, 1:100), anti-nestin antibody (MilliporeSigma; 1:100), anti-collagen II mouse monoclonal antibody (Santa Cruz Biotechnology; 1:50), and rabbit anti-DMP1 antibody (provided by Dr. Chunlin Qin at Texas A&M University, 1:400). Immunoreactivity detection was done by a 3, 3-diaminobenzidine kit (Vector Laboratories, Burlingame, CA, USA). The detection for TUNEL was done by a kit from Millipore (S7100; Temecula, CA, USA). Alkaline phosphatase (ALP) activity was measured by an ALP Assay Kit (Roche, Indianapolis, IN, USA).

2.4. Cell proliferation

EdU (5-ethynyl-2'-deoxyuridine, Life technique, and 10mg/ml) was injected (at 3ml/gm once, based on body weight, 2 hours before sacrifice, i.p.). EdU^+ cells in proliferating layers of mandibular condylar cartilage were counted using Image J software [32].

2.5. Tissue clearing, confocal microscopy and image analysis

Mandibular condyles used for 3-D reconstruction images and movies were collected at 7-week. Tissue clearing was performed on these samples with the PEGASOS method as previously described [33]. Fluorescence cell images were captured using SP5 Leica confocal microscope. All images were obtained at light ranging from 488 (green)-561 (red) μm. Multiple stacked images were taken at 200Hz (1024×1024) and shot in 10X, 20X and 63X objectives [34]. Red Tomato reporter represented *Col* 10a1-Cre^{+} cells and their daughter cells; green color indicated the immunofluorescent staining; blue color showed DAPI staining. Image processing and 3-D reconstruction images and movies were used with Image J software and Imaris 9.0 (Bitplane) [33].

2.6. Serum biochemical analysis

After anesthetizing the mice, blood samples were collected from heart puncture, and then separate serum samples were obtained after precipitation and centrifugation. Serum biochemical analysis was performed to measure the serum level of phosphorus (Pi), FGF-23, calcium (Ca). We measured intact FGF23 levels using a murine iFGF23 ELISA that measures the intact active protein exclusively (Quidel, Immutopics, Carlsbad, CA). We measured serum calcium and phosphate using colorimetric assays (Pointe Scientific, Canton, MI).

2.7. Statistical Analysis

All data were reported as mean ± SEM. Student's t-test was used to detect significance between the age-matched control and *Dmp1* KO groups and oneway ANOVA and Tukey's Test for multiple comparisons were used for Control and *Dmp1* KO with or without High-Pi diet groups. The level of significance was assumed as *$p < 0.05$; **$p < 0.01$. GraphPad Prism 6 (GraphPad Software, Inc.) was used for data analyses.

3. RESULTS

3.1. *Dmp1* knockout (KO) mice develop a drastically malformed TMJ condyle phenotype, which progresses with aging.

Because *Dmp1* KO newborns displayed no obvious skeletal phenotype [35], we focused on *Dmp1* KO mandibular condyles phenotypes postnatally from 10-day to 1-year of age. X-ray images showed no apparent difference between KO and control at age of 10, but gradual changes of condylar shape and size, such as a largely lack of calcified condyle head, uneven mineral content and expanded condylar ramus (Fig. 1a, *right panels*). By the ages of 1-year, the defects of condylar head were greatly exacerbated, including the absence of calcified cartilage head, malformed and porous subchondral bone, and an expanded ramus neck displayed by a photograph and μCT images (Fig. 1b, *right panels*). Safranin O staining showed drastic increases in all layers of chondrocytes and smeared-like immature subchondral bone underneath at the age of P14 (Fig. 1c; *right panel*). Toluidine blue stain revealed a continuous expansion of cartilage and bone mass in 1-year-old KO condyles. Furthermore, there were a high level of alkaline phosphatase (ALP) in the 10-day-old KO hypertrophic zone and subchondral bone area, (Fig. 1e–f; *right panels*), and increased

proliferating cells in the KO prechondroblastic layers (Fig. 1g). However, TUNEL assay showed no significant difference between control and KO cartilage cells (data not shown). These findings demonstrated an essential role of DMP1 in both condyle formation and remodeling, and also suggest that the KO chondrocyte is highly active, challenging a previous view that a slowdown in chondrogenesis and a failure of replacement of hypertrophic chondrocytes by bone cells [36].

3.2. Conditional removing *Dmp1* in chondrocytes by Col10a1-Cre has no apparent impact on condylar morphology

Previously, we reported a restricted expression of DMP1 in hypertrophic chondrocytes [25]. To investigate whether the condyle phenotype in *Dmp1* null mice is caused by a direct role of removing *Dmp1* in these cells, we conditionally removed *Dmp1* in the hypertrophic chondrocyte by crossing the *Dmp1*-loxP mice [23] to *Col10a1-Cre* mice [24]. The X-ray images of the conditional KO condyles displayed no notable differences compared to the age matched controls at ages of 2-, 3- and 7-weeks, although the conventional *Dmp1* KO showed the predicted defect (Fig. 2a–c; *lower panels*). Similarly, Safranin O stained images revealed no change in the cKO condyles compared to the controls at ages of 2-week (Fig. 2d; *right panel*) and 3-weeks (Fig. 2e; *right panel*). This work clearly indicated that the hypertrophic chondrocyte-originated DMP1 in the condyle cartilage may not be essential for hypertrophic-chondrogenesis and cartilage matrix formation.

3.3. Accelerated chondrogenesis and cell-trans-differentiation from hypertrophic chondrocytes to bone cells in the *Dmp1* KO condyle

We and others have shown expanded growth plates and retarded long bone growth in Hyp mice (Phex mutations, equivalent to the same PHEX mutations in XLH patients)[37, 38], *Dmp1* KO mice [8, 15], and DMP1 KO rabbits [9]. A failure in replacement of hypertrophic chondrocytes by bone cells was widely used for explanation why the onset of rickets occurs. However, a recent cell lineage tracing study from our lab demonstrated that the cell trans-differentiation from chondrocytes to bone cells is responsible for TMJ condylar bone growth, which raised a critical issue on the cause of this defective phenotype: whether hypophosphatemia change chondrogenesis or the cell trans-differentiation or both. To precisely address the above issue, we generated two compound mouse lines combine the *Dmp1* KO line with either Acan-Cre^{ERT2}; R26R^{Tomato} (one-time tamoxifen injection at day3 P3 with animals harvested at P10, 3-weeks and 7-weeks, respectively) or Col10a1-Cre; R26R^{Tomato} (Col10al-Cre began to become activated around E14.5, a marker for hypertrophic chondrocytes). The former line was used to address whether removing *Dmp1* changes entire chondrogenesis, and the latter line used to test whether a deletion of *Dmp1* changes hypertrophic-chondrogenesis and the cell trans-differentiation.

Removing *Dmp1* in the Acan tracing line combined with IHC showed a massive increase in Aggrecan^{+} chondrocytes in all three developmental stages analyzed (Fig. 3, right panels). This result demonstrated an accelerated chondrogenesis in the *Dmp1* KO condyle, instead of an inhibition of chondrogenesis as commonly believed.

Due to a low level activity of the R26 promoter in chondrocytes [19], the Col10a1-Cre-R26RTomato red hypertrophic chondrocytes were largely undetected, whereas the red bone cells were observed in the entire 7-week-old WT subchondral bone (Fig. S1a, *left panel*). For better defining the initial Col10a1-Cre- R26RTomato red signal in chondrocytes, we stained the same slide with antibodies against this red fluorescent protein (RFP, green color to distinguish its natural red color). We clearly showed the RFP expression in hypertrophic chondrocytes (Fig. S1a, *mid and right panels*). Interestingly, strong red and green signals of RFP were observed not just in the KO subchondral bone but also in the expanded hypertrophic chondrocyte zone, indicating an accelerated chondrogenesis in the KO (Fig. S1b).

Furthermore, analyses of cartilage and bone molecular marker revealed a sharp increase in SOX9 in both cartilage and bone of the KO condyle (Fig. 4a, *right panel*). Similarly, strong Runx2 signal was detected in both cartilage and bone of the KO condyle (Fig. 4b, *right panel*). These changes were statistically significant (Fig. 4e for SOX9, and Fig 4f for Runx2). In contrast, there was a significant reduction in an expression of SOST (a marker for mature osteocyte) in the KO subchondral bone, indicating that these chondrocyte-derived bone cells are immature (Fig. 4c, g, *right panel*). Furthermore, Col 10 was trapped in the KO hypertrophic chondrocytes, suggesting a defect in protein secretion (Fig. 4d, *right panels*). Taken together, the above data strongly support the notion that there is an acceleration in both chondrogenesis and osteogenesis in the KO condyle. The data also demonstrated a great increase in the cell trans-differentiation of the KO hypertrophic chondrocytes to immature bone cells, instead of an inhibition of both chondrogenesis and osteogenesis as commonly believed.

3.4. Blocking FGF23 function greatly improves *Dmp1* KO condyle phenotype

Having excluded the direct role of DMP1 in condylar hypertrophic chondrocytes, we then analyzed the *Dmp1* KO condyles with and without treatment of neutralizing antibodies against FGF-23, a key causative factor in the onset of hypophosphatemic rickets [5, 10]. Both X-ray and toluidine blue staining images revealed a drastic improvement in the *Dmp1* KO condyle phenotype at two age groups after continuous antibody injections (Fig. 5a; one-week treatment; 5b; three-week treatment). Data support a critical role of phosphorous levels in condylar endochondral bone formation.

3.5. A high-Pi diet treatment significantly improves mineralization and cartilage layer thickness in the *Dmp1* KO condyle

Because of the direct causative role of a low phosphorous on long bone endochondrogenesis [25], the KO and control mice were fed with a High-Pi diet from day 10 to 7-week. As expected, approximately 11-fold increase in serum FGF23 was displayed in *Dmp1* KO mice compared with control mice. And a high-Pi diet fully rescued the Pi level, with no significant difference on the serum Ca (Fig. S2; n=4, *$P < 0.05$, **$P < 0.01$), which is identical to what we reported before [15]. Representative μ-CT images showed a restoration of the calcified condylar head with greatly improved bone quality in the KO+High-Pi group (Fig. 6a). The quantitative μ-CT data demonstrated that a significant reduction in the bone mineral density (BMD), bone volume density (BV/TV), trabecular number (Tb. N), and a

significant increase trabecular separation (Tb. Sp) in the 7-week KO compared to the age matched control group. After a High-Pi diet treatment, the above pathological changes in bone qualities were significantly improved to a level similar to that in the control group (Fig. 6b; n=4, *P < 0.05, **P < 0.01). Similarly, safranin-O stained images clearly displayed drastically improve in cartilage layer thickness in KO mice after a 39-day high-Pi treatment (Fig. 6c; n=4, *P < 0.05, **P < 0.01).

3.6.1. A high-Pi diet treatment restored cartilage residues and rescued an abnormal β-catenin expression in *Dmp1* KO condyle—

Similarly, Sirius red stain images revealed a sharp reduction in cartilage residue productions in the KO group (Fig 7a, *right panel*), which was largely restored by a high-Pi diet treatment (Fig 7a, *middle panel*). On the other hand, the polarized light images showed the greatly increased collagen type I in the KO bone matrix (Fig 7b, *right panel*), and a restoration of this abnormal change to a similar level as that in the control by a High-Pi treatment (Fig. 7b, *middle panel*). Moreover, there was a great increase in the β-catenin level in both the KO hypertrophic chondrocytes and subchondral bone cells (Fig. 7c, *right panel*), which was completely rescued in High-Pi diet KO mice (Fig. 7c, *middle panel*). These data likely support the notion that low Pi increases the level of β-catenin in the KO hypertrophic chondrocytes, which is directly linked to a great expansion of cartilage layers and immature bone formation.

3.6.2. There was an inhibition of extracellular matrix secretion in the KO condyle, which was largely rescued by a high Pi-diet treatment.—

For better understanding the extracellular matrix protein change in the KO condyle, we performed immunohistochemistry assays in the Col 10a1-Cre-tracing line (see Fig. 4 for detail). There was a sharp increase in both the *Col* 10a1-Cre^{+} red chondrocytes and widely spread Col 10 expression in these cells but not in the KO matrix (Fig. 7d, *right panel*). A high Pi diet treatment drastically reduced the Col 10a1^{+} cell numbers and increased Col 10 secretion in the rescued matrix (Fig. 7d, *middle panel*). Similarly, there was an increase in the Col 1 production in the KO cells (Fig. 7e, *right panel*), which was largely restored in the high Pi-diet treated group (Fig. 7e, *middle panel*). Together, these findings suggested an acceleration of chondrogenesis and osteogenesis, and an inhibition of ECM secretion in the KO mice, which is directly associated with the Pi-level.

3.7. The constitutive expression of β-catenin in chondrocytes inhibits ECM secretions.

An association of inhibition of ECM secretion in *Dmp1* KO chondrocytes (Fig. 4d; *right panel*) and a sharp increase in β-catenin (Fig. 7c; *right panel*) raised a likely inhibition role of β-catenin in ECM secretion. To test this hypothesis, we examined levels of the following ECM proteins: Col 1, Col 2, DMP1, and Nestin (Fig. 8; Fig S4) in the compound mice containing Acan-Cre^{ERT2}; CA-β-cat; R26R^{Tomato}. All these proteins were trapped in the CA-β-cat chondrocytes or bone cells, supporting the inhibitory role of CA-β-cat in ECM secretion.

4. DISCUSSION

Short stature and bone deformities are main features of hypophosphatemic rickets in human [39]. Cephalometric studies by Al-Jundi and co-workers also showed that patients with hypophosphatemic rickets have reduced mandibular length and height and deficiency in ramus height among Jordanian children because of the affected TMJ development (age 2–16 years) [40, 41]. In this study, we showed that the *Dmp1* KO mice developed drastic changes in both condylar morphology and mineralization similar to *Dmp1* KO long bone phenotypes in mice and rabbits. Especially, these phenotypes worse with aging. However, the KO hypertrophic-chondrogenic phenotype is directly caused by a reduction of low Pi but not by a loss of *Dmp1* in the chondrocytes based on the following two experiments: 1) Col 10a1-Cre; *Dmp1*$^{fx/fx}$ mice display no apparent change in overall condyle morphology and mineralization (Fig. 2); and 2) admissions of FGF23 neutralizing antibodies or high Pi-diet largely restore the KO condyle phenotype (Figs. 5).

For a long time, the hypophosphatemic rickets was thought to be caused by a failure of replacement of chondrocytes by bone cells, leading to an accumulation of a large cartilage mass and a short malformed skeleton [36]. A recent breakthrough in cell lineage tracing studies precisely demonstrates a direct trans-differentiation of chondrocytes into bone cells in both long bone and mandibular condyle [17–19]. In this study, we demonstrated that a low Pi level accelerate chondrogenesis and cell trans-differentiation of chondrocytes to bone cells (instead of inhibition) in the KO condyle by the following two pieces of evidence: 1) significant increases in ALP enzyme activity and cell proliferation in the KO chondrocytes and bone cells (Fig. 1); and 2) a massive increase in Aggrecan-Cre^{+} or *Col* 10a1-Cre^{+} red chondrocytes and bone cells (Fig. 3–4). However, these increased Aggrecan-Cre^{+} or *Col* 10a1-Cre^{+} red bone cells are immature (as evidenced by a lack of expression of SOST, a marker for mature osteocytes) as DMP1 is required for bone cell maturation [5]. Currently, we do not know why chondrogenesis, but not osteogenesis, is highly sensitive to changes of phosphorus levels. Our speculation is that cartilage is avascular and nutrients can only reach these cells through their matrices (rich in proteoglycan and elastin fibers). In contrast, bone is rich in vessels, and a change in Pi has limited impact on bone cells.

The Wnt/β-catenin pathway plays an essential role in the skeletal formation and development [42, 43]. Previous studies showed that activation of β-catenin in osteoblast increases early osteoblast differentiation but inhibit the trans-differentiation of late stage osteoblast to mature osteocyte, leading to immature bone mass [44–46]. Recent evidence also demonstrated that β-catenin is vital for the cell trans-differentiation of chondrocytes into bone cells during mandibular condylar development [26]. Here, we found that a direct link of the Pi level and β-catenin, and a negative relationship between β-catenin levels and ECM secretion status: a low level of Pi leads to a high level of β-catenin, which directly inhibits ECM secretion in cartilage, and vice versa (Figs. 7–8).

We previously reported that *Dmp1* KO long bones displayed a unique osteoarthritis-like phenotype via the axis of “FGF23-renal phosphorus reabsorption”, including a biphasic change of a articular cartilage (an early expansion and late shrinkage), cartilage degradation, osteophyte formation, and subchondral osteosclerosis [25]. These phenotypes are similar to

long bone phenotypes observed in Hyp mice and mice overexpressing FGF2 [47]. However, the *Dmp1* KO condyle displayed a continuous expansion of cartilage and immature subchondral bone formation, supporting the unique feature of TMJ condyle different from the large joints.

5. Conclusion

The current study demonstrated that the loss of DMP1 leads to a severe defect of condyle development and remodeling, although there is a lack of the direct role of DMP1 in condylar hypertrophic- chondrogenesis. Administrations of the anti-FGF23 neutralizing antibodies or a high Pi diet greatly improved the KO condylar phenotype. Importantly, we demonstrated that hypophosphatemia leads to a sharp increase in acceleration of chondrogenesis (instead of the inhibition of chondrogenesis as commonly believed) and a cell trans-differentiation from chondrocytes to bone cells, and a great reduction of extracellular matrix secretion due to an increase in β-catenin (Figs. 9). Based on these new findings, we propose a new hypothesis to challenge the current view on the onset of hypophosphatemic rickets in the KO mandibular condyle.

Supplementary Material

Refer to Web version on PubMed Central for supplementary material.

ACKNOWLEDGMENT

We thank Jingya Wang for expert SEM techniques. We are grateful to Diane Chen for her assistance with the editing of this article. This study was partly supported by U.S. National Institutes of Health grants to J.Q.F. (R01DE025014 and DE025659), and by China scholarship council to H.L. (201706240157). All authors state that they have no conflicts of interests.

REFERENCES

[1]. Fisher LW, Fedarko NS, Six genes expressed in bones and teeth encode the current members of the SIBLING family of proteins, Connective tissue research 44 Suppl 1 (2003) 33–40. [PubMed: 12952171]

[2]. Fisher LW, Torchia DA, Fohr B, Young MF, Fedarko NS, Flexible structures of SIBLING proteins, bone sialoprotein, and osteopontin, Biochemical and biophysical research communications 280(2) (2001) 460–5. [PubMed: 11162539]

[3]. Ravindran S, George A, Multifunctional ECM proteins in bone and teeth, Exp Cell Res 325(2) (2014) 148–54. [PubMed: 24486446]

[4]. George A, Sabsay B, Simonian PA, Veis A, Characterization of a novel dentin matrix acidic phosphoprotein. Implications for induction of biomineralization, The Journal of biological chemistry 268(17) (1993) 12624–30. [PubMed: 8509401]

[5]. Feng JQ, Ward LM, Liu S, Lu Y, Xie Y, Yuan B, Yu X, Rauch F, Davis SI, Zhang S, Rios H, Drezner MK, Quarles LD, Bonewald LF, White KE, Loss of DMP1 causes rickets and osteomalacia and identifies a role for osteocytes in mineral metabolism, Nat Genet 38(11) (2006) 1310–5. [PubMed: 17033621]

[6]. Feng JQ, Huang H, Lu Y, Ye L, Xie Y, Tsutsui TW, Kunieda T, Castranio T, Scott G, Bonewald LB, Mishina Y, The Dentin matrix protein 1 (Dmp1) is specifically expressed in mineralized, but not soft, tissues during development, Journal of dental research 82(10) (2003) 776–80. [PubMed: 14514755]

[7]. Lorenz-Depiereux B, Bastepe M, Benet-Pages A, Amyere M, Wagenstaller J, Muller-Barth U, Badenhoop K, Kaiser SM, Rittmaster RS, Shlossberg AH, Olivares JL, Loris C, Ramos FJ, Glorieux F, Vikkula M, Juppner H, Strom TM, DMP1 mutations in autosomal recessive hypophosphatemia implicate a bone matrix protein in the regulation of phosphate homeostasis, Nat Genet 38(11) (2006) 1248–50. [PubMed: 17033625]

[8]. Ye L, Mishina Y, Chen D, Huang H, Dallas SL, Dallas MR, Sivakumar P, Kunieda T, Tsutsui TW, Boskey A, Bonewald LF, Feng JQ, Dmp1-deficient mice display severe defects in cartilage formation responsible for a chondrodysplasia-like phenotype, The Journal of biological chemistry 280(7) (2005) 6197–203. [PubMed: 15590631]

[9]. Liu T, Wang J, Xie X, Wang K, Sui T, Liu D, Lai L, Zhao H, Li Z, Feng JQ, DMP1 Ablation in the Rabbit Results in Mineralization Defects and Abnormalities in Haversian Canal/Osteon Microarchitecture, J Bone Miner Res 34(6) (2019) 1115–1128. [PubMed: 30827034]

[10]. Lu Y, Feng JQ, FGF23 in skeletal modeling and remodeling, Curr Osteoporos Rep 9(2) (2011) 103–8. [PubMed: 21404002]

[11]. Carpenter TO, Shaw NJ, Portale AA, Ward LM, Abrams SA, Pettifor JM, Rickets, Nature reviews. Disease primers 3 (2017) 17101. [PubMed: 29265106]

[12]. Feng JQ, Clinkenbeard EL, Yuan B, White KE, Drezner MK, Osteocyte regulation of phosphate homeostasis and bone mineralization underlies the pathophysiology of the heritable disorders of rickets and osteomalacia, Bone 54(2) (2013) 213–21. [PubMed: 23403405]

[13]. Insogna KL, Briot K, Imel EA, Kamenicky P, Ruppe MD, Portale AA, Weber T, Pitukcheewanont P, Cheong HI, Jan de Beur S, Imanishi Y, Ito N, Lachmann RH, Tanaka H, Perwad F, Zhang L, Chen CY, Theodore-Oklota C, Mealiffe M, San Martin J, Carpenter TO, A. Investigators, A Randomized, Double-Blind, Placebo-Controlled, Phase 3 Trial Evaluating the Efficacy of Burosumab, an Anti-FGF23 Antibody, in Adults With X-Linked Hypophosphatemia: Week 24 Primary Analysis, J Bone Miner Res 33(8) (2018) 1383–1393. [PubMed: 29947083]

[14]. Carpenter TO, Imel EA, Ruppe MD, Weber TJ, Klausner MA, Wooddell MM, Kawakami T, Ito T, Zhang X, Humphrey J, Insogna KL, Peacock M, Randomized trial of the anti-FGF23 antibody KRN23 in X-linked hypophosphatemia, J Clin Invest 124(4) (2014) 1587–97. [PubMed: 24569459]

[15]. Zhang R, Lu Y, Ye L, Yuan B, Yu S, Qin C, Xie Y, Gao T, Drezner MK, Bonewald LF, Feng JQ, Unique roles of phosphorus in endochondral bone formation and osteocyte maturation, J Bone Miner Res 26(5) (2011) 1047–56. [PubMed: 21542006]

[16]. Perwad F, Portale AA, Burosumab Therapy for X-Linked Hypophosphatemia and Therapeutic Implications for CKD, Clin J Am Soc Nephrol 14(7) (2019) 1097–1099. [PubMed: 31171590]

[17]. Zhou X, von der Mark K, Henry S, Norton W, Adams H, de Crombrugghe B, Chondrocytes transdifferentiate into osteoblasts in endochondral bone during development, postnatal growth and fracture healing in mice, PLoS genetics 10(12) (2014) e1004820. [PubMed: 25474590]

[18]. Yang L, Tsang KY, Tang HC, Chan D, Cheah KS, Hypertrophic chondrocytes can become osteoblasts and osteocytes in endochondral bone formation, Proceedings of the National Academy of Sciences of the United States of America 111(33) (2014) 12097–102. [PubMed: 25092332]

[19]. Jing Y, Zhou X, Han X, Jing J, von der Mark K, Wang J, de Crombrugghe B, Hinton RJ, Feng JQ, Chondrocytes Directly Transform into Bone Cells in Mandibular Condyle Growth, Journal of dental research 94(12) (2015) 1668–75. [PubMed: 26341973]

[20]. Jing Y, Jing J, Ye L, Liu X, Harris SE, Hinton RJ, Feng JQ, Chondrogenesis and osteogenesis are one continuous developmental and lineage defined biological process, Sci Rep 7(1) (2017) 10020. [PubMed: 28855706]

[21]. Shen G, Darendeliler MA, The adaptive remodeling of condylar cartilage---a transition from chondrogenesis to osteogenesis, J Dent Res 84(8) (2005) 691–9. [PubMed: 16040724]

[22]. Hinton RJ, Serrano M, So S, Differential gene expression in the perichondrium and cartilage of the neonatal mouse temporomandibular joint, Orthod Craniofac Res 12(3) (2009) 168–77. [PubMed: 19627518]

[23]. Feng JQ, Scott G, Guo D, Jiang B, Harris M, Ward T, Ray M, Bonewald LF, Harris SE, Mishina Y, Generation of a conditional null allele for Dmp1 in mouse, Genesis 46(2) (2008) 87–91. [PubMed: 18257058]

[24]. Gebhard S, Hattori T, Bauer E, Schlund B, Bosl MR, de Crombrugghe B, von der Mark K, Specific expression of Cre recombinase in hypertrophic cartilage under the control of a BAC-Col10a1 promoter, Matrix biology : journal of the International Society for Matrix Biology 27(8) (2008) 693–9. [PubMed: 18692570]

[25]. Zhang Q, Lin S, Liu Y, Yuan B, Harris SE, Feng JQ, Dmp1 Null Mice Develop a Unique Osteoarthritis-like Phenotype, Int J Biol Sci 12(10) (2016) 1203–1212. [PubMed: 27766035]

[26]. Jing Y, Jing J, Wang K, Chan K, Harris SE, Hinton RJ, Feng JQ, Vital Roles of beta-catenin in Trans-differentiation of Chondrocytes to Bone Cells, Int J Biol Sci 14(1) (2018) 1–9. [PubMed: 29483820]

[27]. Brault V, Moore R, Kutsch S, Ishibashi M, Rowitch DH, McMahon AP, Sommer L, Boussadia O, Kemler R, Inactivation of the beta-catenin gene by Wnt1-Cre-mediated deletion results in dramatic brain malformation and failure of craniofacial development, Development 128(8) (2001) 1253–64. [PubMed: 11262227]

[28]. Fen JQ, Zhang J, Dallas SL, Lu Y, Chen S, Tan X, Owen M, Harris SE, MacDougall M, Dentin matrix protein 1, a target molecule for Cbfa1 in bone, is a unique bone marker gene, J Bone Miner Res 17(10) (2002) 1822–31. [PubMed: 12369786]

[29]. Jing Y, Hinton RJ, Chan KS, Feng JQ, Co-localization of Cell Lineage Markers and the Tomato Signal, J Vis Exp (118) (2016).

[30]. Dempster DW, Compston JE, Drezner MK, Glorieux FH, Kanis JA, Malluche H, Meunier PJ, Ott SM, Recker RR, Parfitt AM, Standardized nomenclature, symbols, and units for bone histomorphometry: a 2012 update of the report of the ASBMR Histomorphometry Nomenclature Committee, J Bone Miner Res 28(1) (2013) 2–17. [PubMed: 23197339]

[31]. Jiang X, Kalajzic Z, Maye P, Braut A, Bellizzi J, Mina M, Rowe DW, Histological analysis of GFP expression in murine bone, The journal of histochemistry and cytochemistry : official journal of the Histochemistry Society 53(5) (2005) 593–602.

[32]. Jing J, Hinton RJ, Mishina Y, Liu Y, Zhou X, Feng JQ, Critical role of Bmpr1a in mandibular condyle growth, Connective tissue research 55 Suppl 1 (2014) 73–8. [PubMed: 25158185]

[33]. Jing D, Zhang S, Luo W, Gao X, Men Y, Ma C, Liu X, Yi Y, Bugde A, Zhou BO, Zhao Z, Yuan Q, Feng JQ, Gao L, Ge WP, Zhao H, Tissue clearing of both hard and soft tissue organs with the PEGASOS method, Cell research 28(8) (2018) 803–818. [PubMed: 29844583]

[34]. Ren Y, Lin S, Jing Y, Dechow PC, Feng JQ, A novel way to statistically analyze morphologic changes in Dmp1-null osteocytes, Connective tissue research 55 Suppl 1 (2014) 129–33. [PubMed: 25158197]

[35]. Ye L, MacDougall M, Zhang S, Xie Y, Zhang J, Li Z, Lu Y, Mishina Y, Feng JQ, Deletion of dentin matrix protein-1 leads to a partial failure of maturation of predentin into dentin, hypomineralization, and expanded cavities of pulp and root canal during postnatal tooth development, J Biol Chem 279(18) (2004) 19141–8. [PubMed: 14966118]

[36]. Qin C, D'Souza R, Feng JQ, Dentin matrix protein 1 (DMP1): new and important roles for biomineralization and phosphate homeostasis, J Dent Res 86(12) (2007) 1134–41. [PubMed: 18037646]

[37]. Fuente R, Gil-Pena H, Claramunt-Taberner D, Hernandez-Frias O, Fernandez-Iglesias A, Hermida-Prado F, Anes-Gonzalez G, Rubio-Aliaga I, Lopez JM, Santos F, Marked alterations in the structure, dynamics and maturation of growth plate likely explain growth retardation and bone deformities of young Hyp mice, Bone 116 (2018) 187–195. [PubMed: 30096468]

[38]. Martin A, David V, Li H, Dai B, Feng JQ, Quarles LD, Overexpression of the DMP1 C-terminal fragment stimulates FGF23 and exacerbates the hypophosphatemic rickets phenotype in Hyp mice, Mol Endocrinol 26(11) (2012) 1883–95. [PubMed: 22930691]

[39]. Lambert AS, Linglart A, Hypocalcaemic and hypophosphatemic rickets, Best Pract Res Clin Endocrinol Metab 32(4) (2018) 455–476. [PubMed: 30086869]

[40]. Al-Jundi SH, Al-Naimy YF, Alsweedan S, Dental arch dimensions in children with hypophosphataemic Vitamin D resistant rickets, Eur Arch Paediatr Dent 11(2) (2010) 83–7. [PubMed: 20403302]

[41]. Al-Jundi SH, Dabous IM, Al-Jamal GA, Craniofacial morphology in patients with hypophosphataemic vitamin-D-resistant rickets: a cephalometric study, J Oral Rehabil 36(7) (2009) 483–90. [PubMed: 19531089]

[42]. Duan P, Bonewald LF, The role of the wnt/beta-catenin signaling pathway in formation and maintenance of bone and teeth, The international journal of biochemistry & cell biology 77(Pt A) (2016) 23–29. [PubMed: 27210503]

[43]. Bonewald LF, Johnson ML, Osteocytes, mechanosensing and Wnt signaling, Bone 42(4) (2008) 606–15. [PubMed: 18280232]

[44]. Bao Q, Chen S, Qin H, Feng J, Liu H, Liu D, Li A, Shen Y, Zhong X, Li J, Zong Z, Constitutive beta-catenin activation in osteoblasts impairs terminal osteoblast differentiation and bone quality, Exp Cell Res 350(1) (2017) 123–131. [PubMed: 27865936]

[45]. Jia M, Chen S, Zhang B, Liang H, Feng J, Zong Z, Effects of constitutive beta-catenin activation on vertebral bone growth and remodeling at different postnatal stages in mice, PLoS One 8(9) (2013) e74093. [PubMed: 24066100]

[46]. Chen S, Feng J, Bao Q, Li A, Zhang B, Shen Y, Zhao Y, Guo Q, Jing J, Lin S, Zong Z, Adverse Effects of Osteocytic Constitutive Activation of ss-Catenin on Bone Strength and Bone Growth, J Bone Miner Res 30(7) (2015) 1184–94. [PubMed: 25639729]

[47]. Meo Burt P, Xiao L, Hurley MM, FGF23 Regulates Wnt/beta-Catenin Signaling-Mediated Osteoarthritis in Mice Overexpressing High-Molecular-Weight FGF2, Endocrinology 159(6) (2018) 2386–2396. [PubMed: 29718273]

Highlights:

- DMP1 plays no direct role in hypertrophic chondrogenesis, although hypophosphatemia leads to severe defects in the *Dmp1* KO condyle;
- Hypophosphatemia greatly accelerates condylar chondrogenesis and differentiation of chondrocytes into bone cells;
- Hypophosphatemia directly inhibits condylar extracellular matrix protein secretion via an increase in β-catenin;
- Administrations of antibodies against FGF23 or a high phosphorus diet drastically improve Dmp1 KO condylar phenotype by inhibiting β-catenin levels.

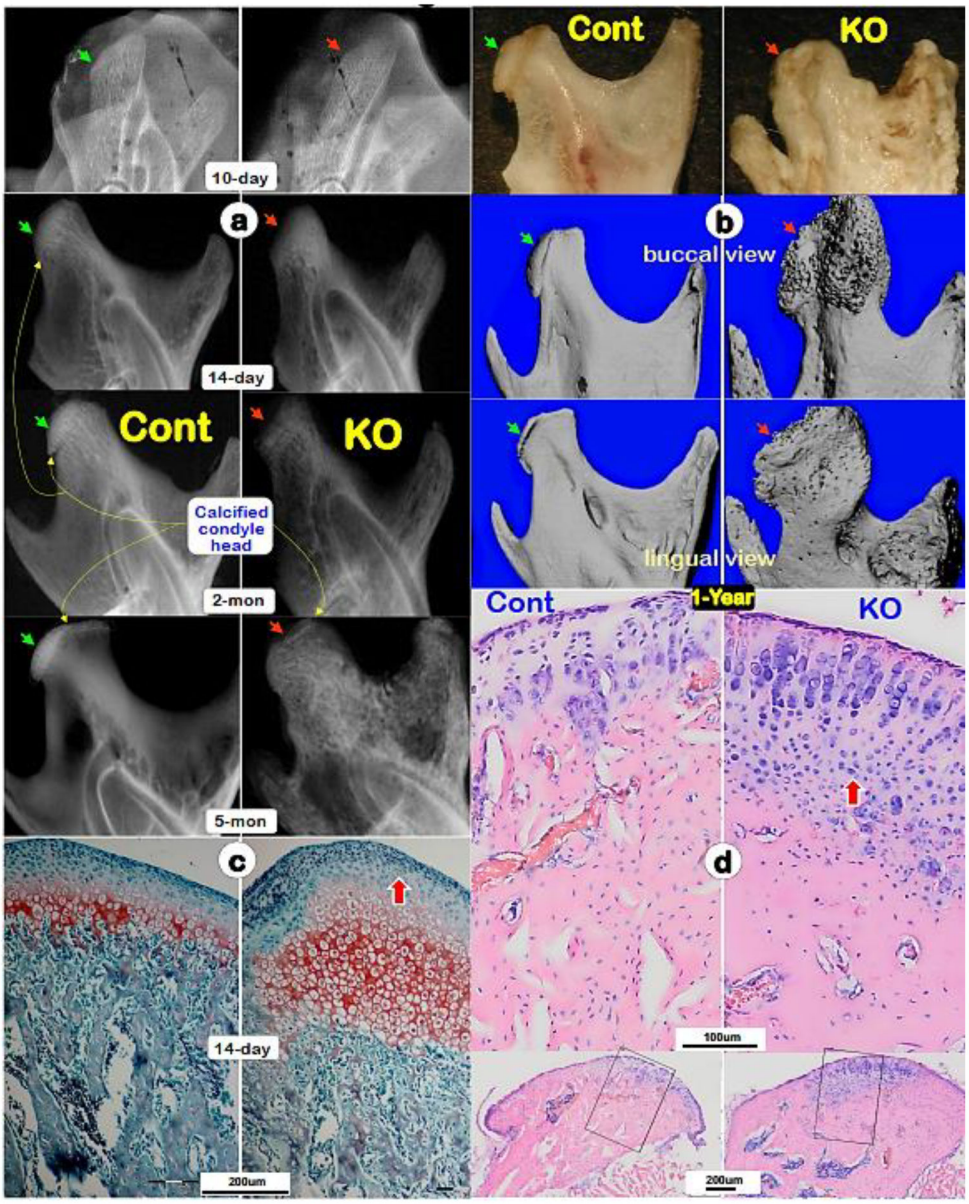

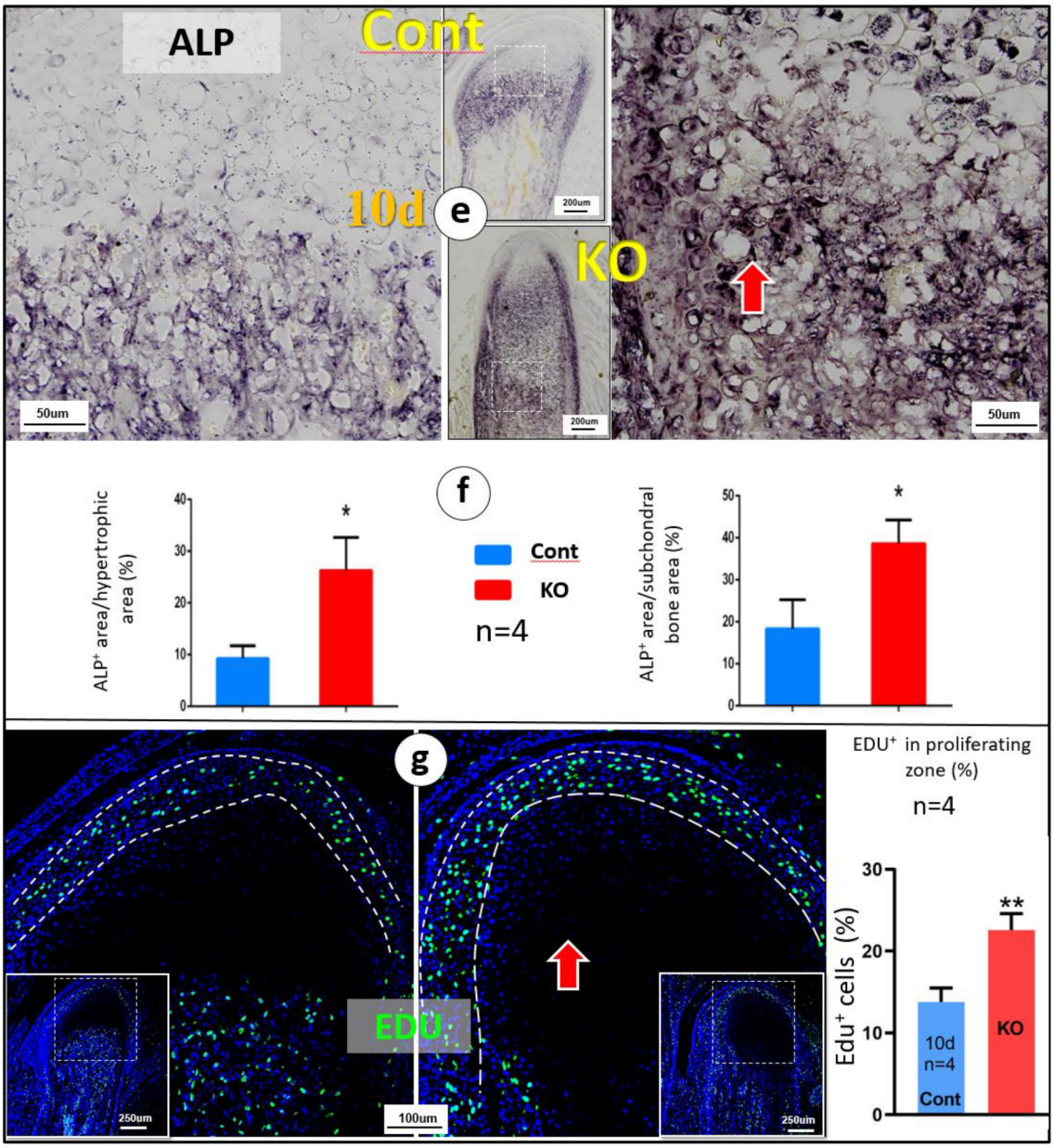

Fig. 1. Progressive changes of *Dmp1* knockout (KO) condyles, which are exacerbated with age.

(a) Representative radiographs of 10-days, 14-days, 2-months and 5-months showed a largely lack of calcified condylar head with poorly formed condylar ramus in KO mice (*right panels*, red arrows) compared to the age matched controls (*left panels;* green arrows). (b) Representative 1-year-old photographs (*top panels*; arrows), Micro-computed tomography (μ-CT) buccal views (*middle panels*; arrows) and μ-CT lingual views (*lower panels*; arrows) displayed great expansions of KO condyle and ramus compared to the age matched controls; (c) Safranin O staining images displayed great expanded hypertrophic area and disorganized subchondral bone in a 14-day-old KO condyle (*right panel*) compared to a control (*left panel*); and(d) Toluidine blue images exhibited a continuous expansion of the KO condylar head at age of one-year (*right panel*) compared to the age matched control (*left panel*).

(e) Alkaline phosphatase (ALP) activity was higher in the 10-day-old KO condyle (*right panel*) compared to the age matched control;(f) Quantitative analyses revealed significant differences of ALP activities between the KO and control in both hypertrophic chondrocyte zone and subchondral bones (n=4; $p < 0.05$); (g) Representative EDU images revealed more proliferated chondrocytes in the KO condyle (right panel); a significant difference of EDU (n=4; $p < 0.01$).

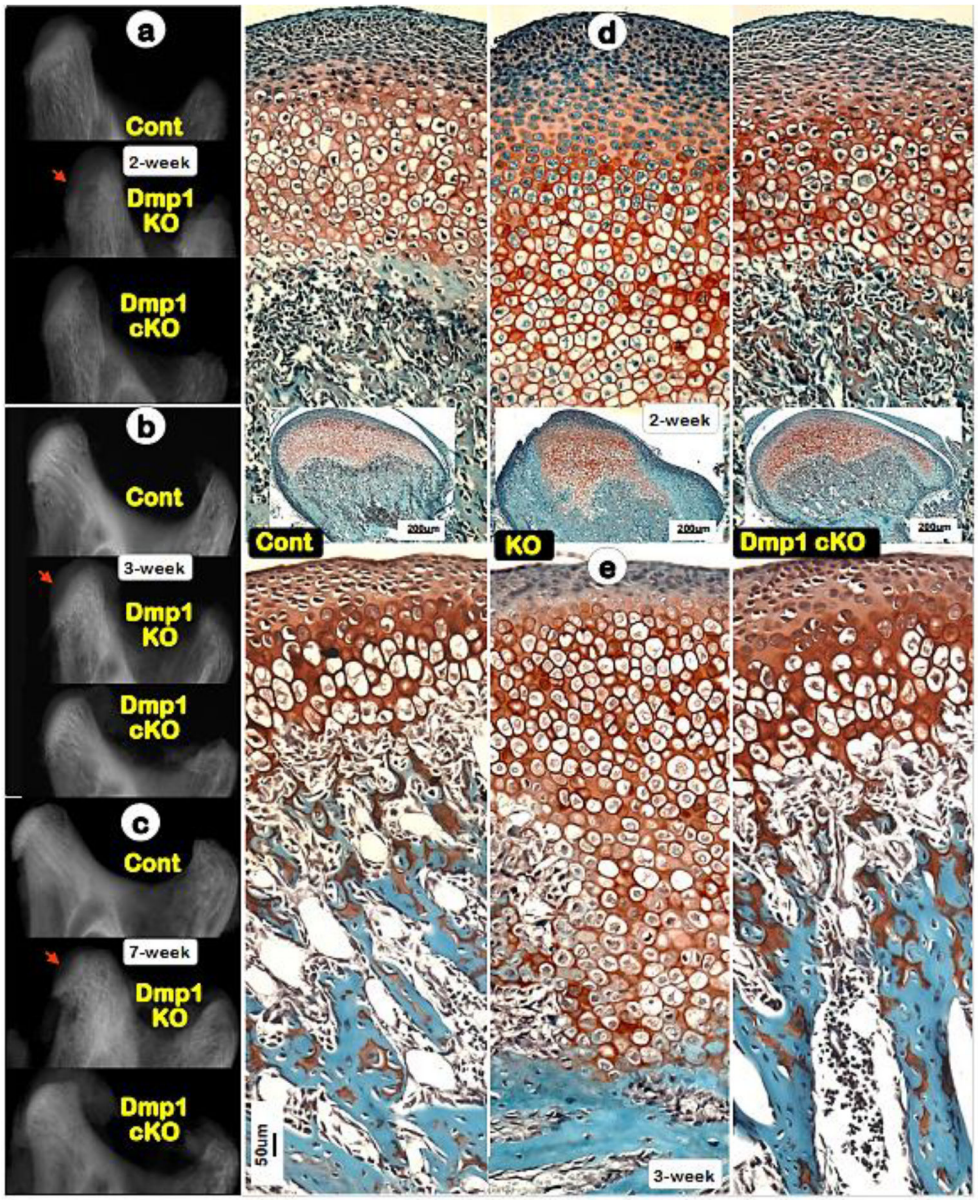

Fig. 2. Deletion of *Dmp1* in hypertrophic chondrocytes results in no apparent impact on condyle morphology.

(a-c) Representative radiograph images revealed striking condyle defects in the conventional *Dmp1* KO mice *(middle panels)*, although the Col10a1-Cre; *Dmp1*$^{fx/fx}$ (*Dmp1* cKO) mice display no dramatic change in its condyle *(lower panels)* at ages of 2-, 3- and 7-week;(d-e) Representative Safranin O stain images showed great expansion of KO cartilage layers *(middle panels)*, whereas the cKO chondrocytes *(right panels)* were largely similar to those in controls of ages of 2- and 3-weeks *(left panels)*

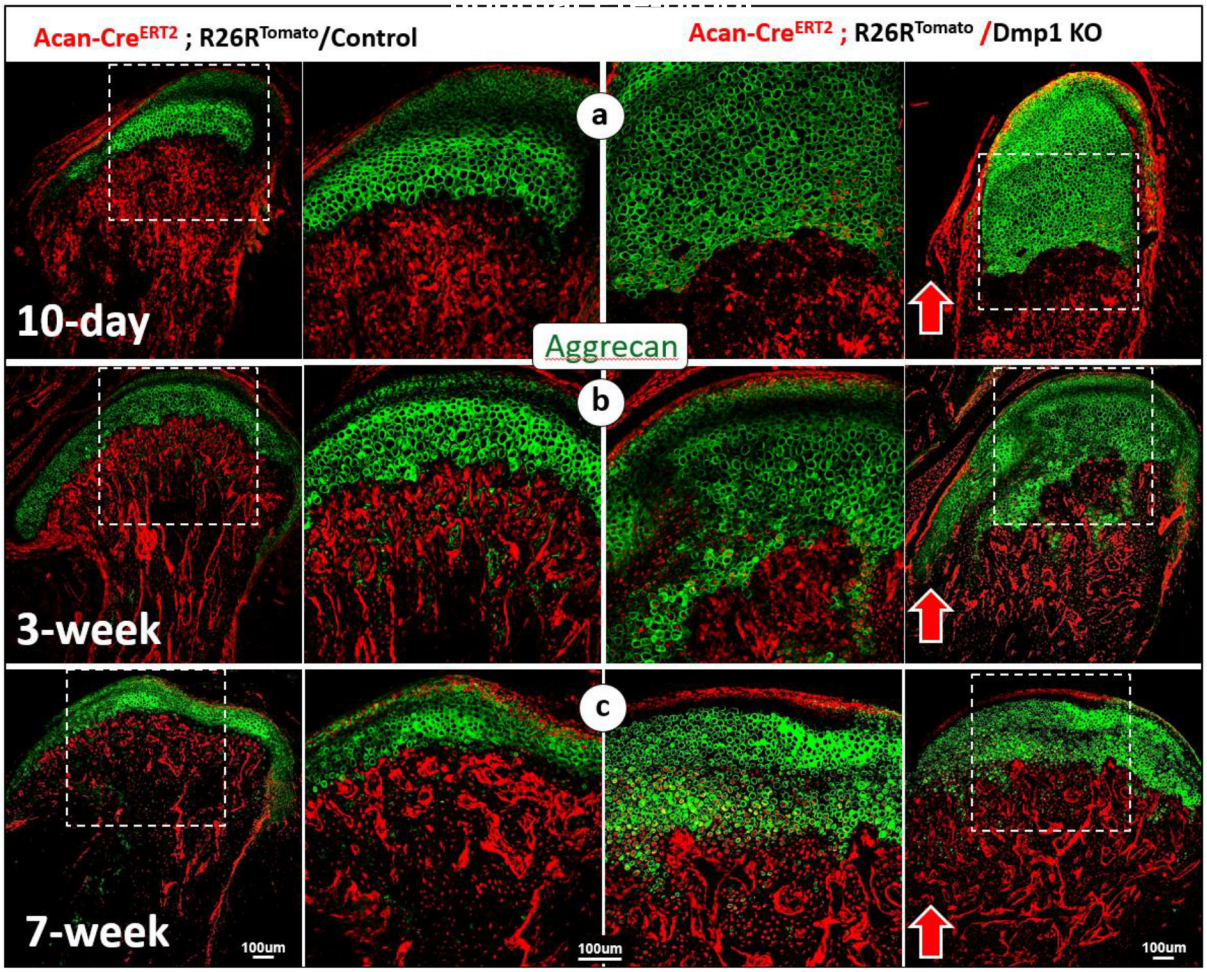

Fig. 3. A sharp increase in Aggcan^{+} chondrocytes and red bone cells in the *Dmp1* KO condyle.

(a-c) Aggrecan IHC combined with cell lineage tracing (Acan-Cre^{ERT2} was activated at P3, tracing the fate of chondrocytes) demonstrated highly expansion of Aggrecan^{+} cartilage area in KO condyles at ages of postnatal 10-days (a, right panels), 3-weeks (b, right panels), and 7-weeks (c, right panels), supporting the notion that there is a great increase in chondrogenesis in *Dmp1* KO condyles.

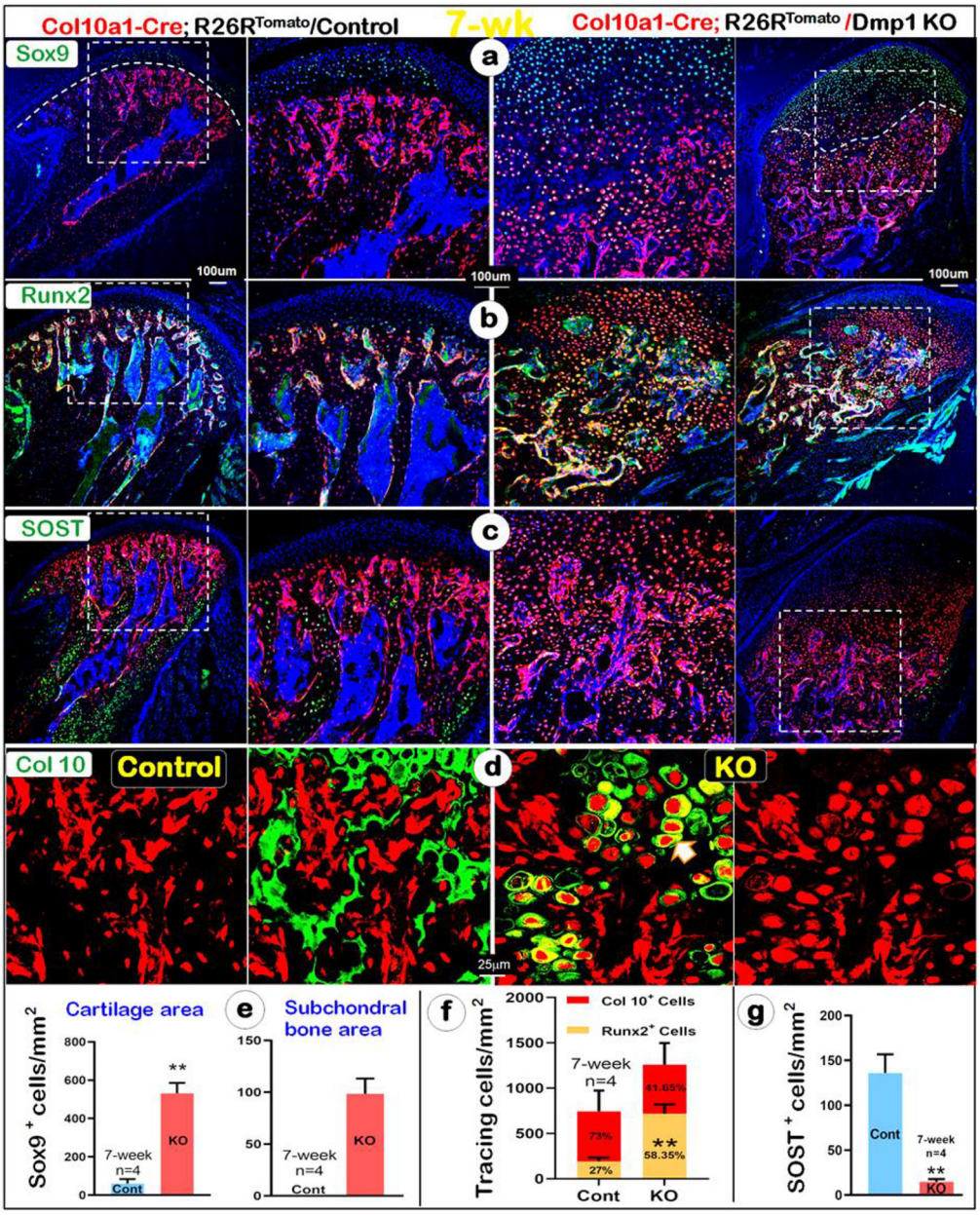

Fig. 4. An acceleration of cell trans-differentiation of hypertrophic chondrocytes to immature bone cells in the 7-week-old KO condyle.

(a-g) There was a sharp increase in the $Sox9^+$ chondrocytes and bone cells in the KO condyle by immunohistochemistry (a, *right panels*); Similarly, there was a drastic increase of Col 10a1-Cre^+/$Runx2^+$ chondrocytes and bone cells in the KO condyle (b, *right panels*); Quantitative data analyses confirmed that these changes are statistically different in $Sox9^+$ chondrocytes and bone cells, white line separating cartilage from bone tissue (e) and Col 10a1-Cre^+/$Runx2^+$ chondrocytes and bone cells (f); n=4, *P < 0.05, **P < 0.01. (c, g) Immunohistochemistry data showed few $SOST^+$ cells (a marker for mature osteocyte) in the KO bone cells, indicating immature bone mass (*right panel*); n=4, *P < 0.05, **P < 0.01 (d)

Immunohistochemistry data revealed a lack of Col 10 secretion in the KO condyle (*right panel*) compared to the control, in which Col 10 was secreted in the ECM (*left panel*).

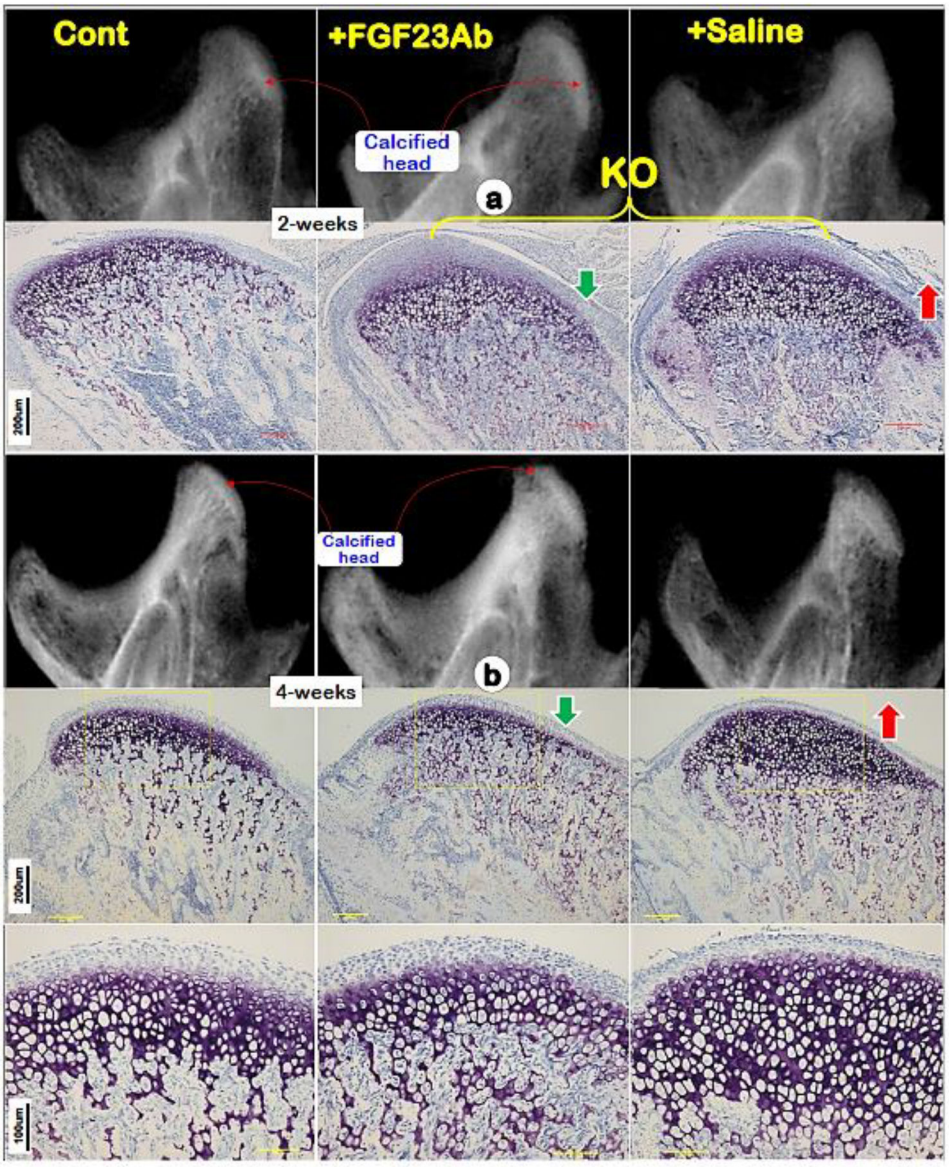

Fig. 5. Restoration of *Dmp1* KO condyle defects using anti-FGF-23 antibody injections.

(a) Representative X-ray *(upper middle panel)* and Toluidine blue stain *(lower middle panel)* images of *Dmp1* KO condyles showed rapid improvement of the KO condyle compared to the saline treated group *(right panels)* after one week treatment of anti-FGF-23 antibodies; (b) Representative X-ray *(upper middle panel)* and Toluidine blue stain *(lower middle panels)* images of *Dmp1* KO condyles showed largely restorations of the KO condyle compared to the saline treated group *(right panels)* after three week treatment of anti-FGF-23 antibodies.

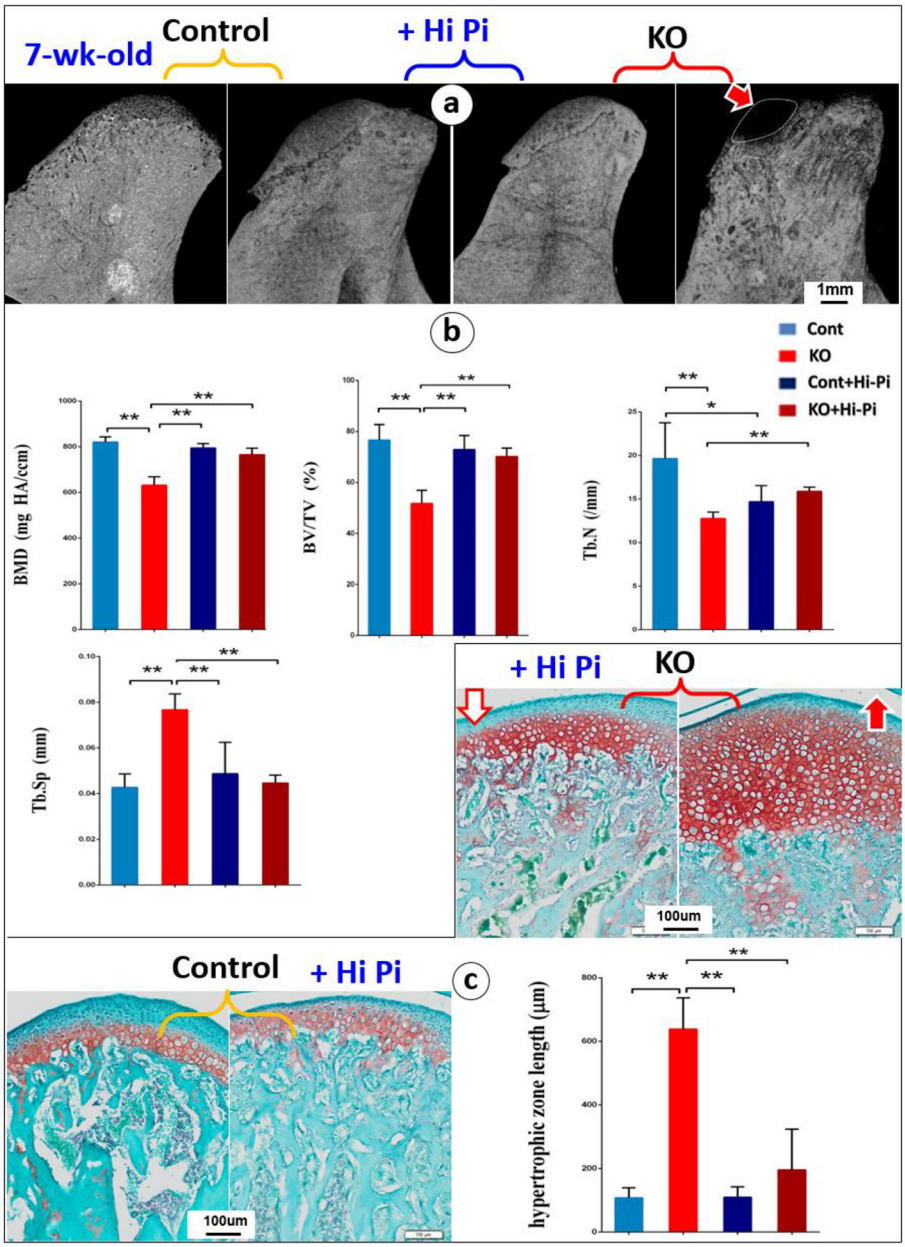

Fig. 6. Restorations of the expanded cartilage layers and immature bone formation by a High-Pi diet treatment started at the age of 10-day and harvested at age of 49-day.

(a-b) Representative μ-CT images of the condyles revealed a full rescue of the calcified condylar head in the treated KO group by a High-Pi diet (a); Quantitative data showed significant improvement of mineralization related parameters, including BMD, BV/TV, Tb.Sp and Tb.N (b);(c) Representative safranin-O stained images showed restoration of cartilage layers in the KO condyle by a High-Pi diet, which is statistically significant, n=4, *P < 0.05, **P < 0.01.

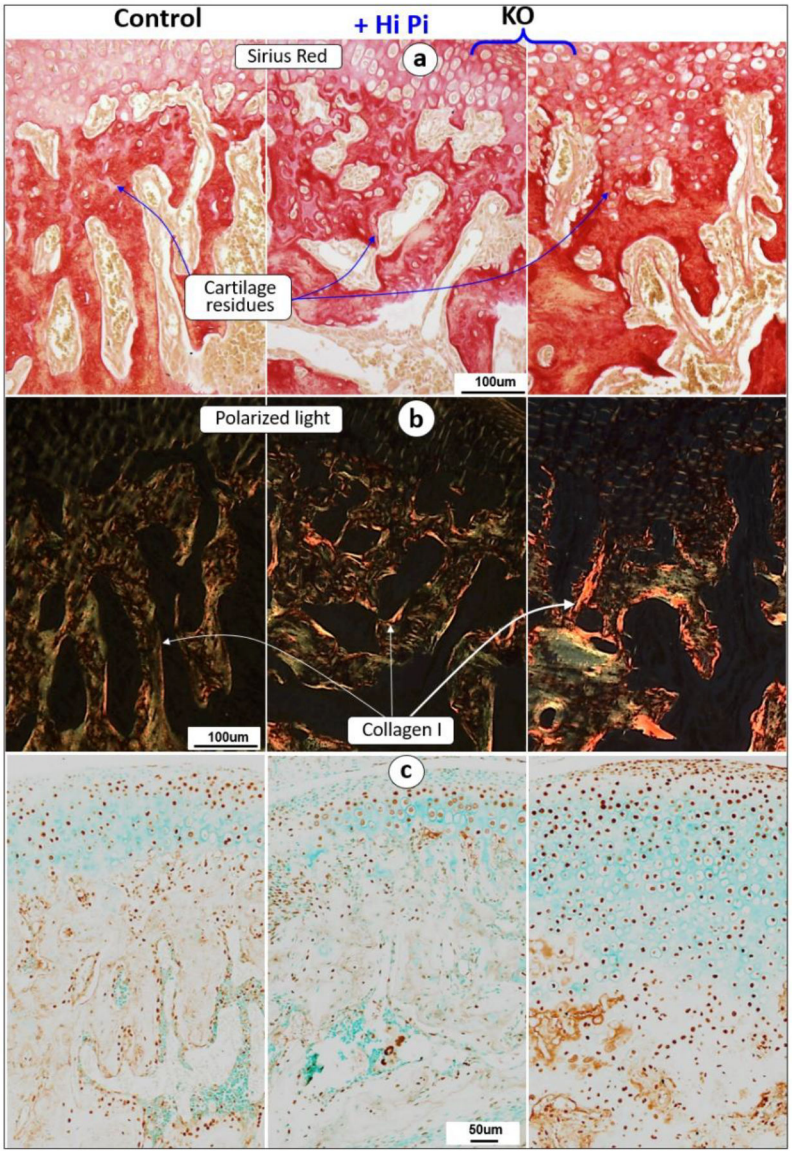

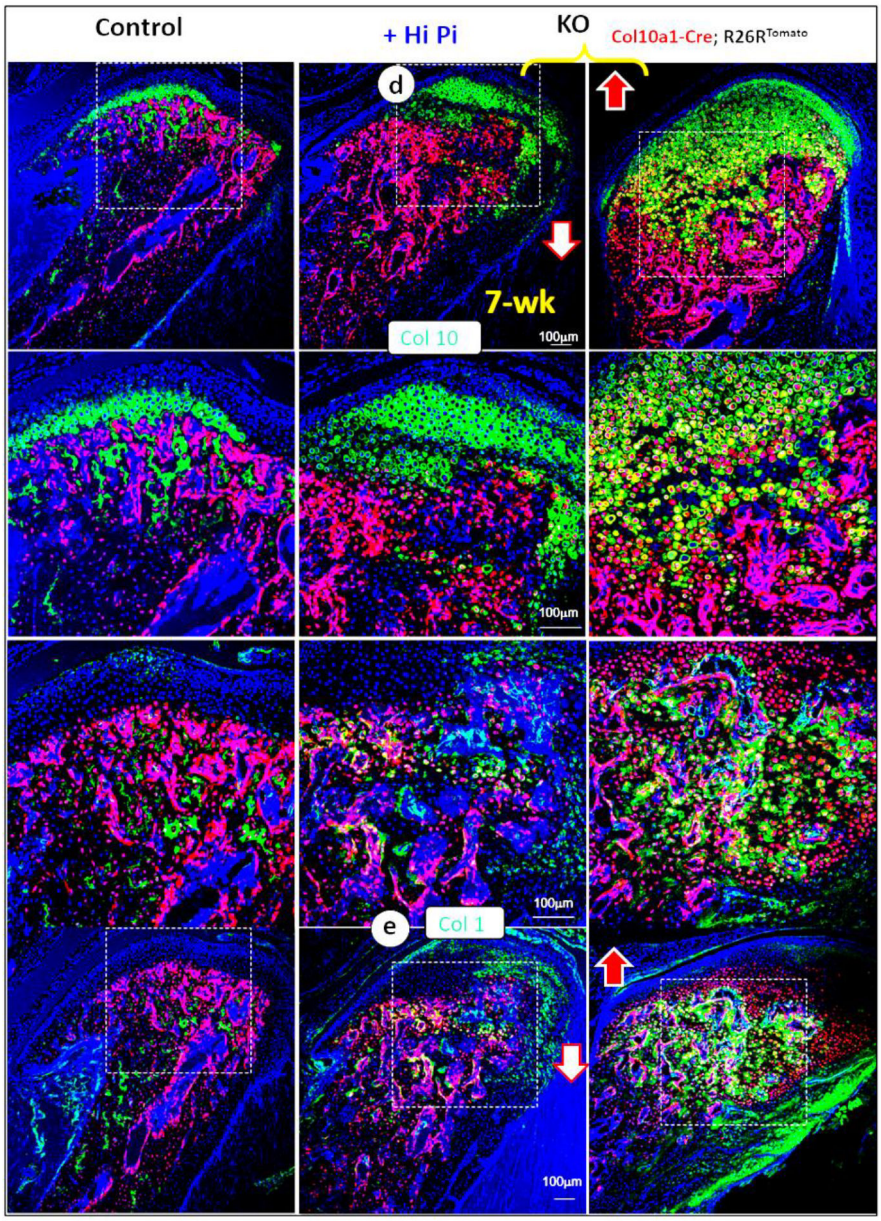

Fig. 7. A high-Pi diet increased cartilage residue secretions and rescued abnormal β-catenin expressions in 7-week old KO mice.

(a-b) The decalcified cross section images of Sirius red stain (a) and the polarized microscopy (b) images showed a full rescue of cartilage residues and decrease in bone matrices in the KO+high-Pi condyle (*middle panels*); (c) The immunohistochemistry images displayed an increase in β-catenin^{+} cells in the entire KO cartilage area (*right panel*), which was fully restored by a High-Pi diet (*middle panel*);

(d-e) Immunohistochemistry data revealed a great improvement of expressions of Col 10 (d, a chondrocyte marker) and Col I (e, a bone marker) in KO condyle by a high Pi diet fully or partially increased ECM in the KO mice, including Col10 and Col 1 (middle panel).

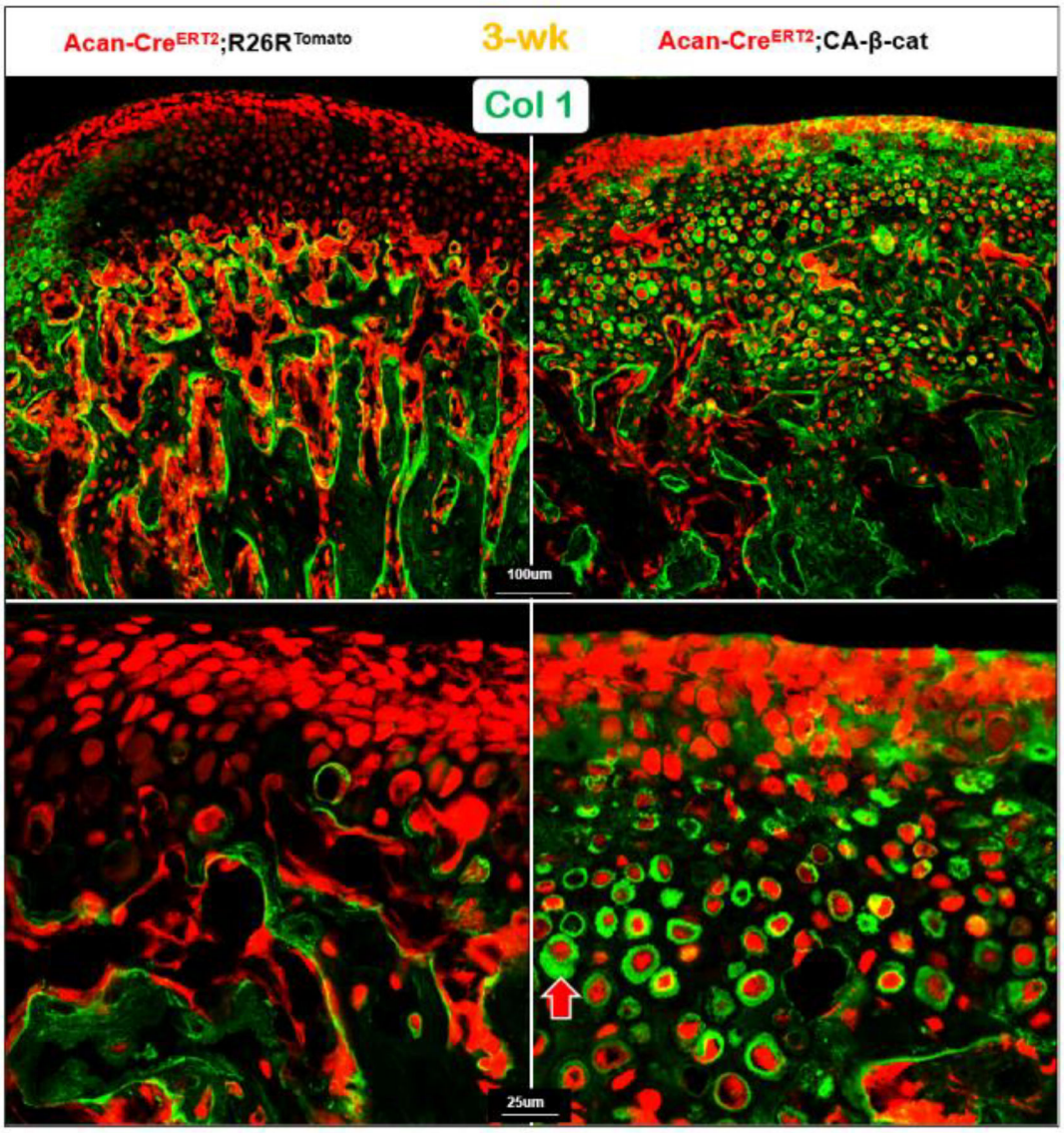

Fig. 8. The targeted activation of β-catenin in chondrocytes result in acceleration of chondrogenesis and cell trans-differentiation, as well as an inhibition of Col I secretion.

The compound mice, containing Acan-Cre^{ERT2}; β-catenin flox$^{(Ex3)}$/flox$^{(Ex3)}$;R26R mice with Cre activation at P3, displayed massive red bone-like cells in the 21-day-old KO condylar cartilage area, in which Col I was trapped in the KO cells (*lower right panel, red arrow*).

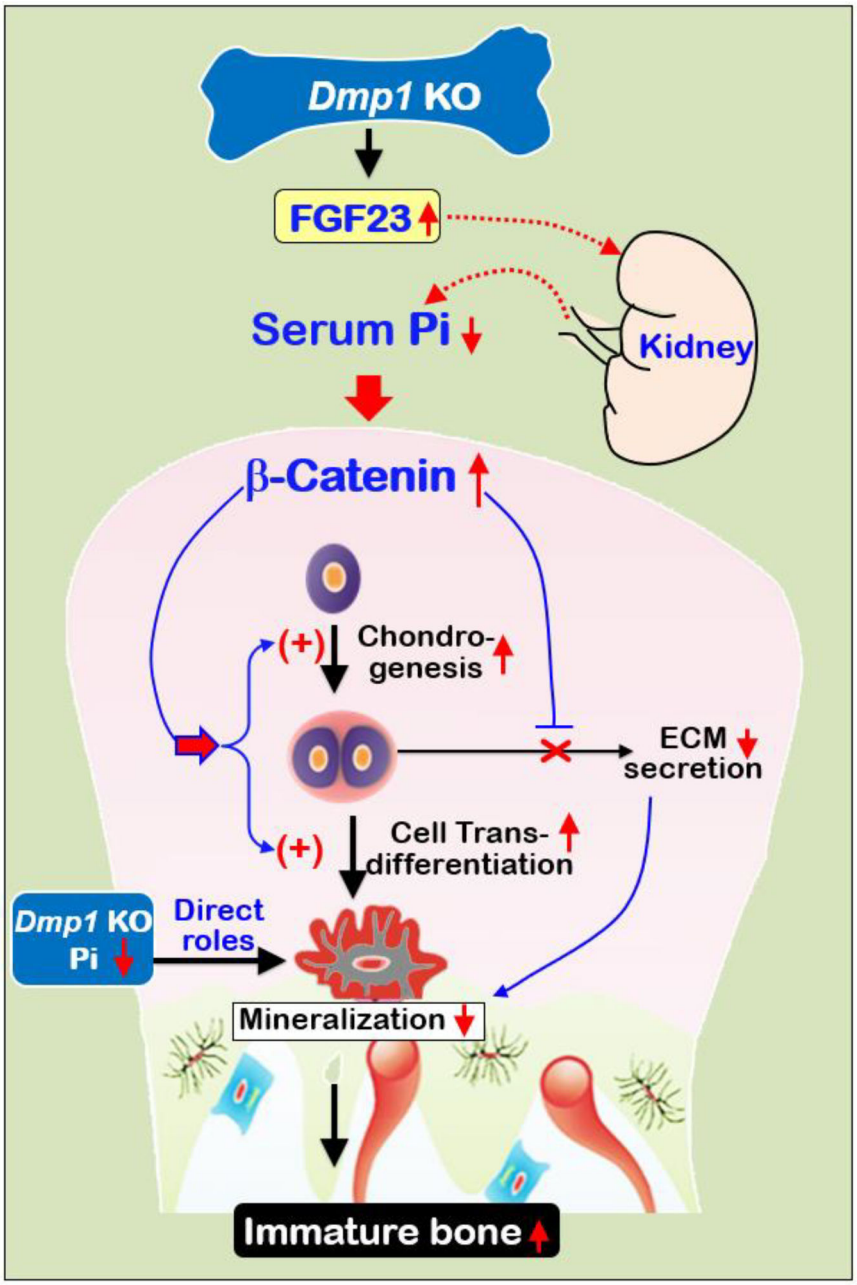

Fig. 9. Working hypotheses.

Removing *Dmp1*, a key ECM molecule released from osteocytes, leads to hypophosphatemia via an increase in FGF23 [5] (Fig. S2). Due to a lack of vasculi in cartilage, a low Pi particularly affects condylar chondrogenesis, leading to a sharp increase in β-catenin in chondrocytes. As a result, both chondrogenesis and cell trans-differentiation from chondrocytes to bone cells are significantly accelerated. However, the increased bone cells remain immature and the KO bone is poorly mineralized due to the direct role of a low Pi (for mineral formation) and a lack of DMP1 (for cell maturation), as well as a reduction in secretions of ECM (where mineral is deposited) caused by the increased β-catenin.